Earthquake Source Inversion with Dense Networks

Surendra Nadh Somala[1], Jean-Paul Ampuero[2], Nadia Lapusta[1,2]

surendra@caltech.edu, ampuero@gps.caltech.edu, lapusta@caltech.edu

[1]Division of Engineering and Applied Sciences, Caltech; [2]Division of Geological and Planetary Sciences, Caltech

1. INTRODUCTION

Inversions of earthquake source slip from the recorded ground motions typically impose a number of restrictions on the source parameterization, which are needed to stabilize the inverse problem with sparse data. Such restrictions may include smoothing, causality considerations, predetermined shapes of the local source-time function, and constant rupture speed. The goal of our work is to understand whether the inversion results could be substantially improved by the availability of much denser sensor networks than currently available. The best regional networks have sensor spacing in the tens of kilometers range, much larger than the wavelengths relevant to key aspects of earthquake physics. Novel approaches to providing orders-of-magnitude denser sensing include low-cost sensors (Community Seismic Network) and space-based optical imaging (Geostationary Optical Seismometer). However, in both cases, the density of sensors comes at the expense of accuracy.

Inversions that involve large number of sensors are intractable with the current source inversion codes. Hence we are developing a new approach that can handle thousands of sensors. It employs iterative conjugate gradient optimization based on an adjoint method and involves iterative time-reversed 3D wave propagation simulations using the spectral element method (SPECFEM3D). To test the developed method, and to investigate the effect of sensor density and quality on the inversion results, we have been considering kinematic and dynamic synthetic sources of several types. In each case, we produce the data by a forward SPECFEM3D calculation, choose the desired density of stations, filter the data to 1 Hz, add noise of the desired level, and then apply our inversion approach.

2. METHODOLOGY & MODEL SETUP

The goal is to minimize Lagrangian

$$\mathcal{L}(\dot{\mathbf{s}},\mathbf{m},\lambda)=\frac{1}{2}\int_0^T\sum_{r=1}^{n}C_D\left[h(t)*\left(\dot{\mathbf{s}}(x_r,y_r,t,\mathbf{m})-\dot{\mathbf{d}}(x_r,y_r,t)\right)\right]^2dt-\int_0^T\int_\Omega \boldsymbol{\lambda}\cdot h(t)*\left(\rho\partial_t^2\dot{\mathbf{s}}-\nabla.(\mathbf{C}:\nabla\dot{\mathbf{s}})-\dot{\mathbf{f}}(\mathbf{m})\right)d^3\mathbf{x}dt$$

Imposing Stationarity

$$0=\frac{\partial\mathcal{L}}{\partial\dot{\mathbf{s}}}\delta\dot{\mathbf{s}}\quad\forall\,\delta\dot{\mathbf{s}}\qquad(1)$$

$$0=\frac{\partial\mathcal{L}}{\partial\mathbf{m}}\delta\mathbf{m}\quad\forall\,\delta\mathbf{m}\qquad(2)$$

$$0=\frac{\partial\mathcal{L}}{\partial\boldsymbol{\lambda}}\delta\boldsymbol{\lambda}\quad\forall\,\delta\boldsymbol{\lambda}\qquad(3)$$

Adjoint Wave Equation

(1) => $$\left[\rho\partial_t^2\mathbf{s}^\dagger-\nabla.(\mathbf{C}:\nabla\mathbf{s}^\dagger)\right]=\sum_r C_D\left[h(T-t)*\left(\dot{\mathbf{s}}(\mathbf{x_r},T-t)-\dot{\mathbf{d}}(\mathbf{x_r},T-t)\right)\right]\delta(\mathbf{x}-\mathbf{x_r})$$

Gradient of Cost Function

(2) => $$\frac{\partial\chi}{\partial\mathbf{m}}\delta\mathbf{m}=\int_0^T\int_\Sigma h(t)\star\mathbf{T}^\dagger(\mathbf{x},T-t)\cdot\delta\mathbf{m}d^2\mathbf{x}dt$$

Forward Wave Equation

(3) => $$\rho\partial_t^2\dot{\mathbf{s}}-\nabla.(\mathbf{C}:\nabla\dot{\mathbf{s}})=\dot{\mathbf{f}}(\mathbf{m})$$

Using gradient information in combination with conjugate-gradient algorithm for asymmetric linear equations and least squares problem (CGLS), we invert for the source (slip rate at a function of space and time)

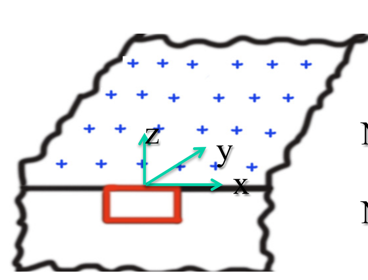

A vertical strike-slip fault embedded in an elastic homogenous half-space with varying network densities and noise levels.

Network Spacing :
1 km to 20 km

Noise Levels :
0 cm/s to 10 cm/s

Magnitude :
Mw 7.0

Coarse Network : 20 km
Dense Network : 1 km
Cutoff frequency : 1Hz

Noise:
Gaussian
Additive
Uncorrelated

(A) Schematic diagram of showing geometry of problem

6. SUMMARY

The results indicate that dense (1 km spacing between stations) networks produce sharper images of the considered sources than sparse (20 km spacing between stations) networks, with better amplitude recovery and better resolution with depth. This is true even when noiseless sparse networks are compared with noisy dense networks, provided that the standard deviations of noise do not exceed ~1% of the maximum earthquake source amplitude. Substantial qualitative improvements arise when features of relatively narrow spatial extent are included in the source, in which case the dense networks can reproduce the features whereas the sparse networks cannot. To avoid distortions in the inverted slip models, one needs to consider the actual 3D velocity models.

3. TRADE OFF BETWEEN NETWORK DENSITY AND NOISE

We considered several kinematic ruptures ranging from simple unilateral pulses to complex ruptures to see if a denser network with noise can invert for the rupture process better than a coarse network that is noiseless. A dynamic rupture scenario is also considered to address this question.

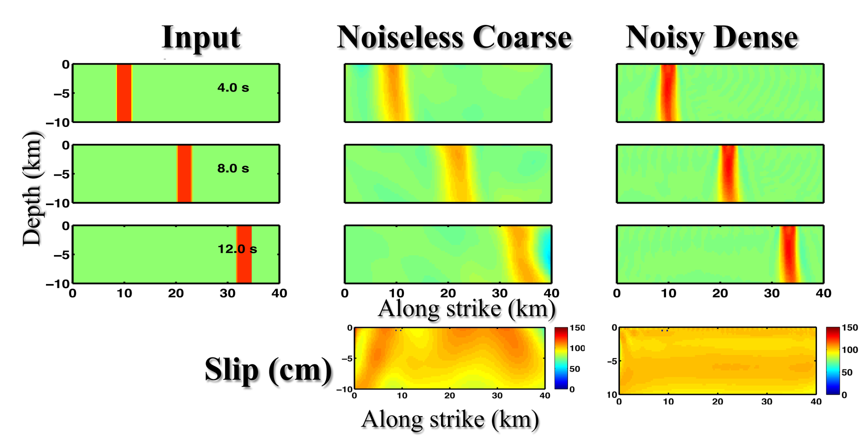

(A) Slip rate and slip of simple Haskell inversion

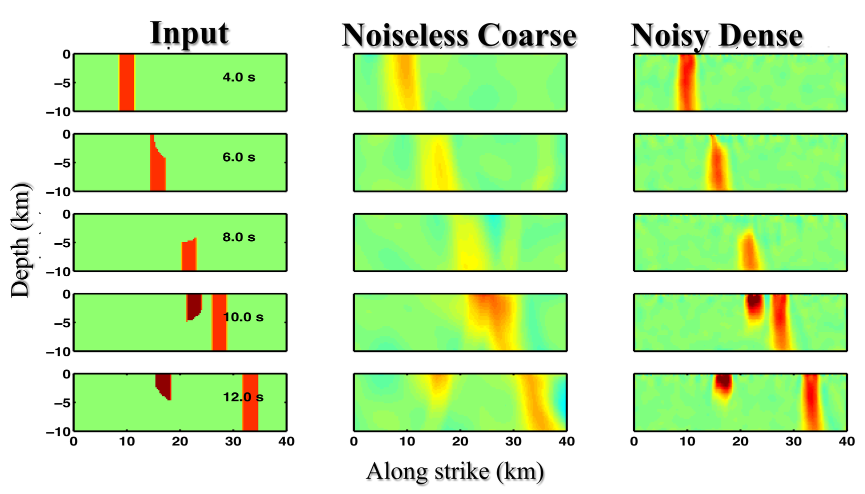

(C) Slip rate of unilateral pulse with a semi-circular asperity that propagates backward

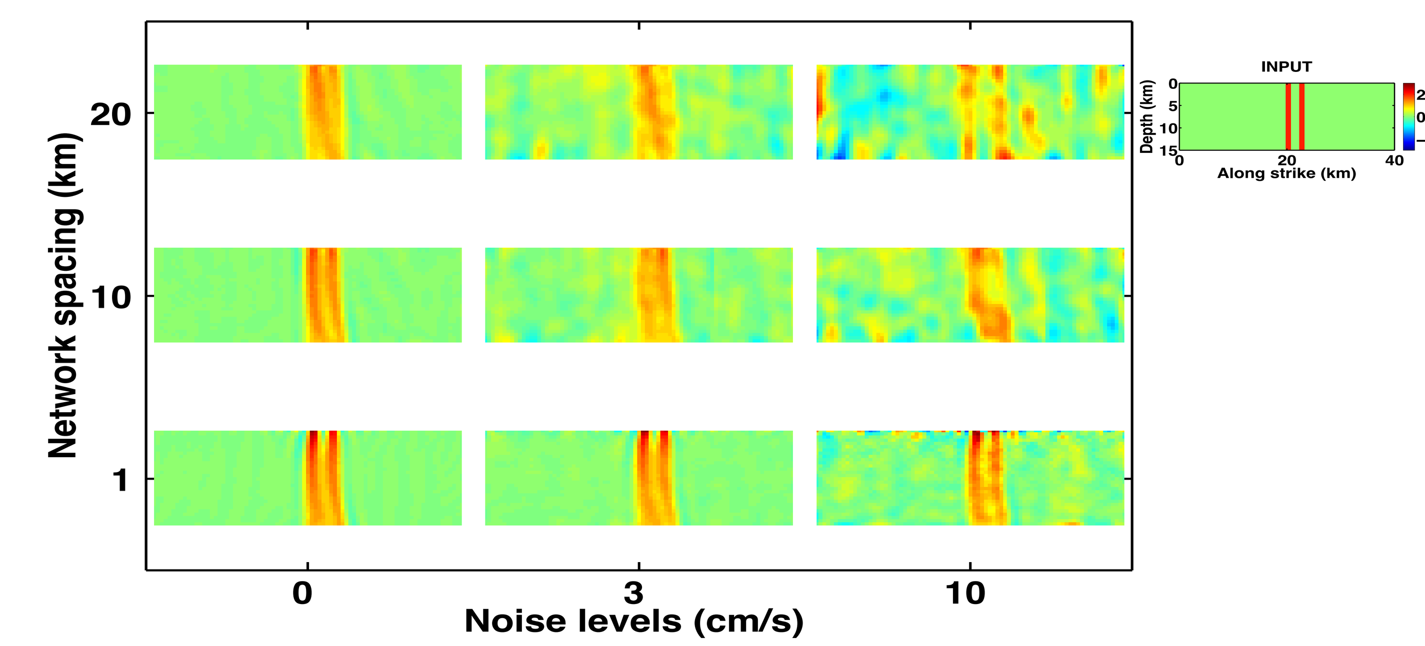

(E) Slip rate of double pulse inversion for different network densities and noise levels

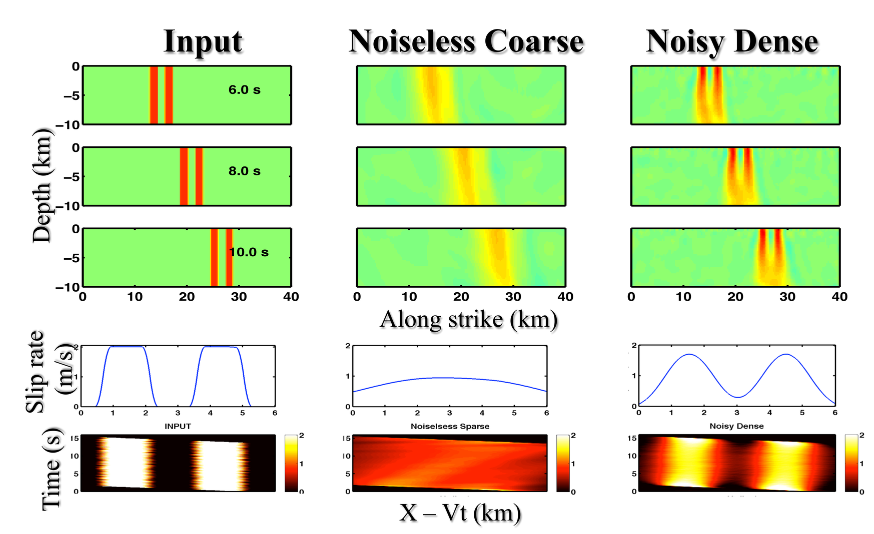

(B) Slip rate of double pulse inversion and its profiles

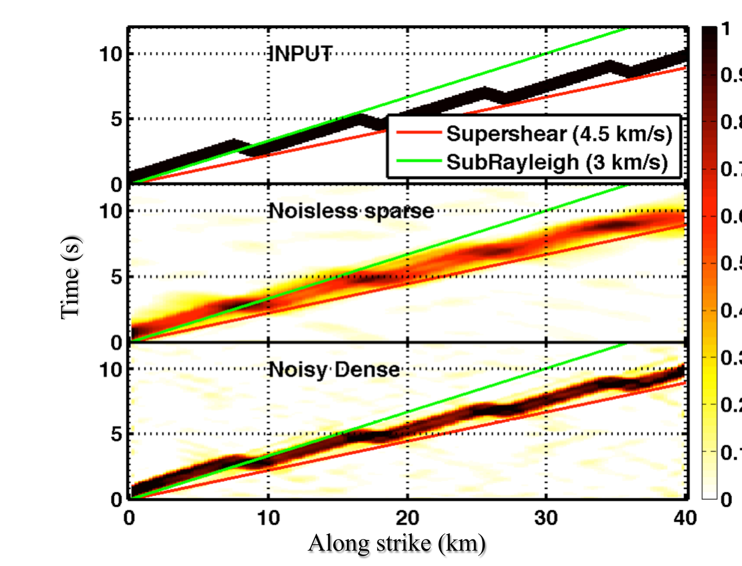

(D) X-T graph of slip rate of sub-Rayleigh pulse that jumps ahead of itself having an overall effective supershear speed

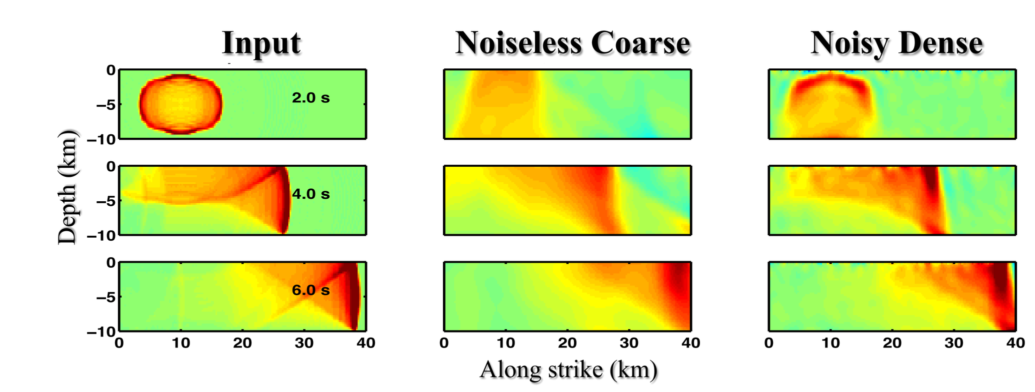

(F) Slip rate of a dynamic rupture (subshear) inversion

5. EFFECT OF UNCERTAINTIES IN VELOCITY MODEL

Using data from a 3D velocity model, we perform inversions with homogeneous velocity as well as 3D velocity model to understand how different the inverted source looks like from input if the 3D structure is not known in detail and how it compares with inversion using the 3D velocity model.

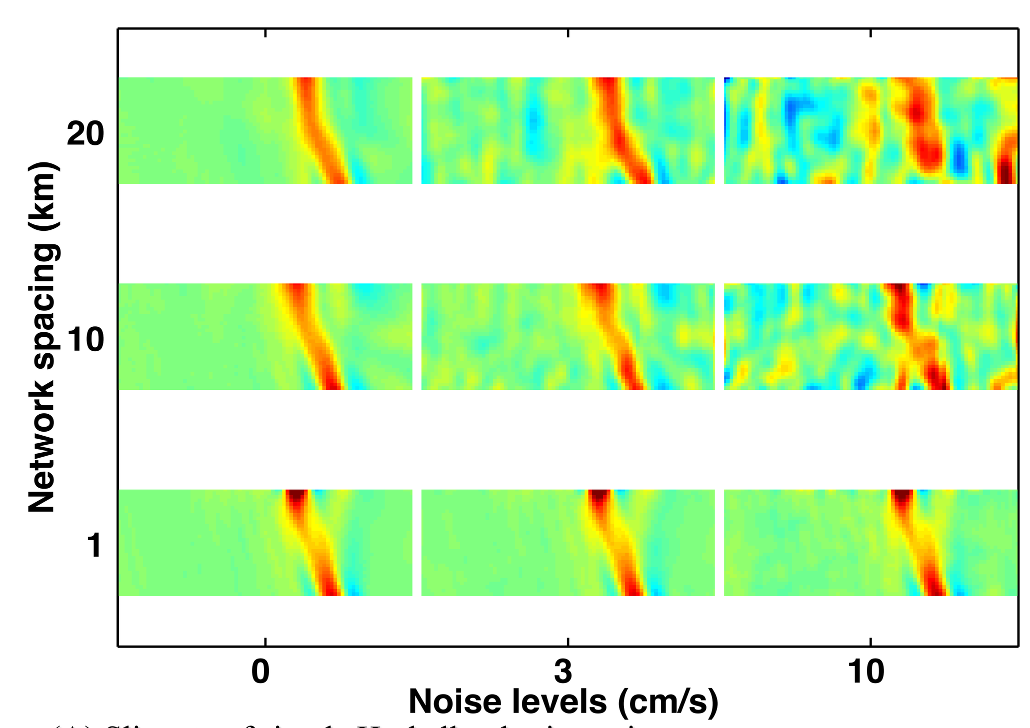

(A) Slip rate of simple Haskell pulse inversion showing tradeoff of noise with network-density

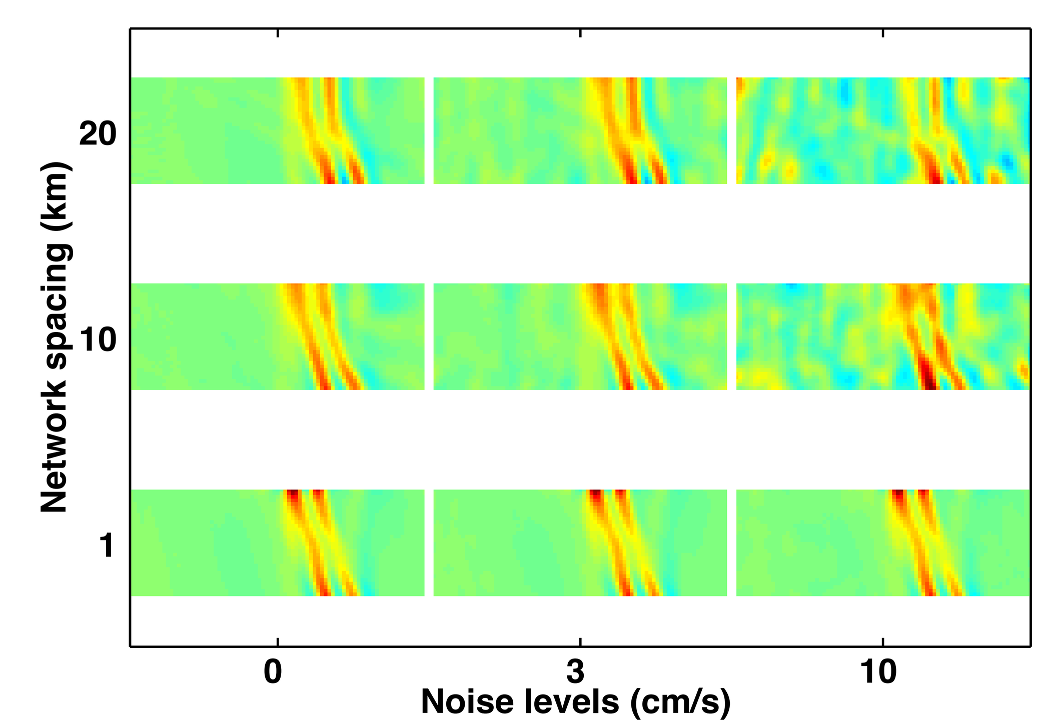

(B) Slip rate of double pulse inversion showing tradeoff of noise with network-density

3D velocity model:
Correlation length 5km
Perturbation 5%
Exponential correlation function

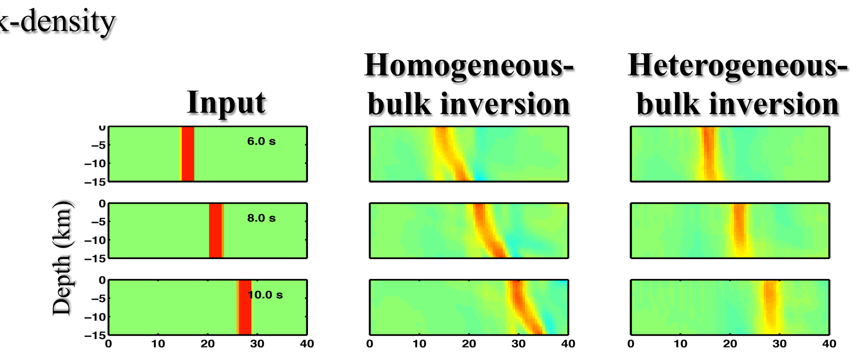

(C) Slip rate of simple Haskell inversion using homogeneous and heterogeneous velocity models during inversion (sparse network)

If the perturbations of velocity structure from background velocity model are not taken into account, a straight pulse can be distorted to the extent that it appears to be bent/curved at the bottom of the fault and at times broken in the middle. This is verified here when background velocity model is homogeneous half-space. We expect similar result for layered velocity model.

4. TESTING RISE TIMES

An input scenario with two pulses but different rise times is considered to see if the inversion shows two pulses irrespective of the network considered.

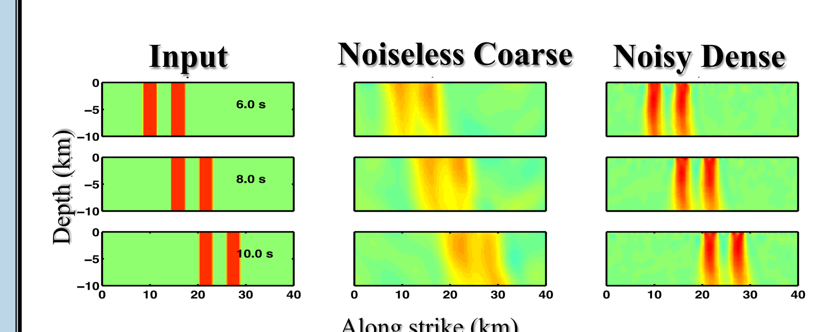

(A) Slip rate of a double pulse inversion with 1 sec rise time separated one pulse width gap

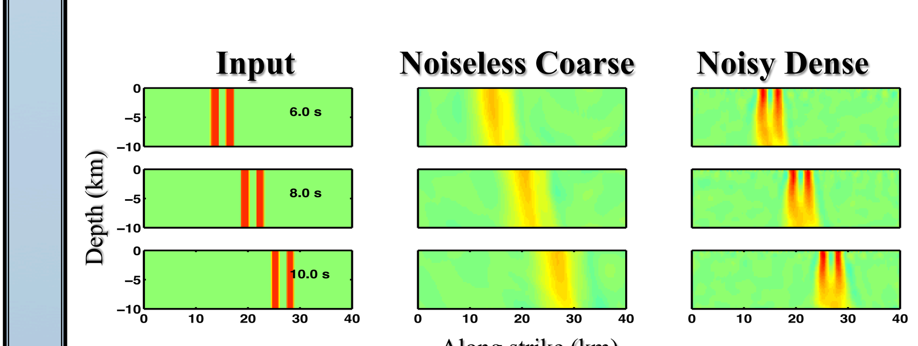

(B) Slip rate of a double pulse inversion with 0.5 sec rise time separated one pulse width gap